4C.8 UPPER-TROPOSPHERIC PRECURSORS ASSOCIATED WITH SUBTROPICAL CYCLONE FORMATION IN THE NORTH ATLANTIC BASIN

Alicia M. Bentley*
University at Albany, SUNY, Albany, New York

1. INTRODUCTION

The National Hurricane Center (NHC) online glossary defines a subtropical cyclone (STC) as a "non-frontal low-pressure system that has characteristics of both tropical and extratropical cyclones…. Unlike tropical cyclones, subtropical cyclones derive a significant portion of their energy from baroclinic sources…often associated with an upper-level low or trough" (OFCM 2013). The NHC definition emphasizes the hybrid nature of STCs and suggests that both baroclinic and diabatic energy sources contribute to STC formation. The duality of baroclinic and diabatic energy sources contributing to STC formation causes STCs to be located somewhere between extratropical cyclones (ECs) and tropical cyclones (TCs) in an idealized cyclone energy source phase space, in which various combinations of baroclinic and diabatic energy sources are used to distinguish between cyclone types (Fig. 1).

Despite the existence of an STC definition in the NHC online glossary, there is currently no objective set of characteristics used to define STCs (Evans and Guishard 2009). In view of the potential for STCs to become TCs via the tropical transition (TT) process (Davis and Bosart 2003, 2004), the lack of an objective set of characteristics used to define STCs motivates this research. The goal of this research is to formulate an objective identification technique for detecting STC formation by quantifying the relative contributions of baroclinic and diabatic processes during the evolution of individual cyclones. This objective identification technique for detecting STC formation will be used to refine the NHC definition of STCs and to construct a North Atlantic STC climatology for 1979–2010. A cyclone-relative composite analysis will also be performed on subjectively constructed clusters of North Atlantic STCs identified in the 1979–2010 climatology to document the structure, motion, and evolution of upper-tropospheric features linked to STC formation.

* *Corresponding author address*: Alicia M. Bentley, University at Albany, SUNY, 1400 Washington Ave., Albany, NY 12222-0100; e-mail: ambentley@albany.edu

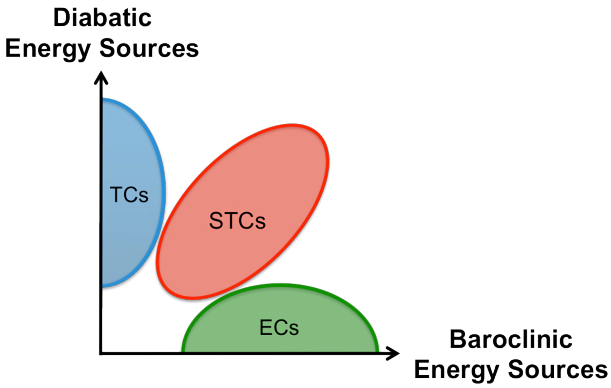

Figure 1. Idealized cyclone energy source phase space diagram [Fig. 9 adapted from Beven (2012)].

2. ADAPTED DAVIS (2010) METHODOLOGY

Several studies examined baroclinically influenced North Atlantic STC and TC development from a physical perspective (e.g., Evans and Guishard 2009; Guishard et al. 2009) and dynamical perspective (e.g., Davis 2010; McTaggart-Cowan et al. 2008, 2013) following the publication of Davis and Bosart (2003, 2004). Davis (2010) was the only study to quantify the relative contributions of baroclinic and diabatic processes during the evolution of individual cyclones and to develop a methodology for identifying STCs within an idealized numerical simulation. The Davis (2010) methodology for STC identification is based on the concepts of Ertel potential vorticity (PV) and is formulated in terms of two PV metrics that quantify the relative contributions of baroclinic processes and condensation heating during the evolution of individual cyclones. The Davis (2010) methodology distinguishes between cyclone types based on the relative contributions of baroclinic processes and condensation heating during the evolution of individual cyclones and can be thought of as similar to the cyclone phase space diagrams developed by Hart (2003).

This research expands upon the work of Davis (2010) by investigating the roles of baroclinic and diabatic processes during the evolution of individual cyclones within the NCEP Climate Forecast System Reanalysis (CFSR) 0.5° gridded dataset (Saha et al. 2010). The transition from identifying STCs within an idealized numerical simulation to the 0.5° CFSR dataset

requires the adaptation of the original Davis (2010) methodology. All PV metrics considered in the present study are calculated in a 6° box centered over the surface cyclone. The first PV metric in the Davis (2010) methodology, PV1, represents lower-tropospheric baroclinic processes in terms of the near-surface potential temperature anomaly:

$$\text{PV1} = g\eta G/\Delta p_1, \tag{1}$$

where

$$G = (G_x^2 + G_y^2)^{1/2},$$

$$G_x = \frac{1}{L_{xc}} \int_{-\frac{L_y}{2}}^{\frac{L_y}{2}} \theta' dy\Big|_{x=\frac{L_x}{2}} - \frac{1}{L_{xc}} \int_{-\frac{L_y}{2}}^{\frac{L_y}{2}} \theta' dy\Big|_{x=-\frac{L_x}{2}},$$

$$G_y = \frac{1}{L_y} \int_{-\frac{L_{xn}}{2}}^{\frac{L_{xn}}{2}} \theta' dx\Big|_{y=\frac{L_y}{2}} - \frac{1}{L_y} \int_{-\frac{L_{xs}}{2}}^{\frac{L_{xs}}{2}} \theta' dx\Big|_{y=-\frac{L_y}{2}},$$

η is the absolute vorticity, and θ' is the potential temperature anomaly calculated at an individual grid point from an 11-day centered mean. The potential temperature anomaly variations across the 6° box, G_x and G_y, are averaged between 925 hPa and 850 hPa prior to computing G. L_y is the length of 6° of latitude and L_x is the longitudinal length of the box as a function of latitude. L_{xn}, L_{xc}, and L_{xs} represent the lengths of the northern edge, center, and southern edge of the 6° box, respectively. The vertical scale, Δp_1, is equal to 425 hPa to match the vertical integration of the lower-tropospheric PV anomaly (see below).

The second PV metric in the Davis (2010) methodology, PV2, represents midtropospheric latent heat release in terms of the lower-tropospheric PV anomaly:

$$\text{PV2} = \frac{\int_{-\frac{L_x}{2}}^{\frac{L_x}{2}} dx \int_{-\frac{L_y}{2}}^{\frac{L_y}{2}} dy \int_{500\ hPa}^{925\ hPa} q' dp}{L_{xc} L_y \Delta p_2} \tag{2}$$

where q' is the PV anomaly calculated at an individual grid point from an 11-day centered mean and Δp_2 is equal to 425 hPa.

For the purposes of this study, the author introduces an additional metric, PV3, representing upper-tropospheric dynamical processes in terms of the upper-tropospheric PV anomaly:

$$\text{PV3} = \frac{\int_{-\frac{L_x}{2}}^{\frac{L_x}{2}} dx \int_{-\frac{L_y}{2}}^{\frac{L_y}{2}} dy \int_{200\ hPa}^{500\ hPa} q' dp}{L_{xc} L_y \Delta p_3} \tag{3}$$

where Δp_3 is equal to 300 hPa. A schematic representation of the regions over which PV1, PV2, and PV3 are calculated is shown in Fig. 2.

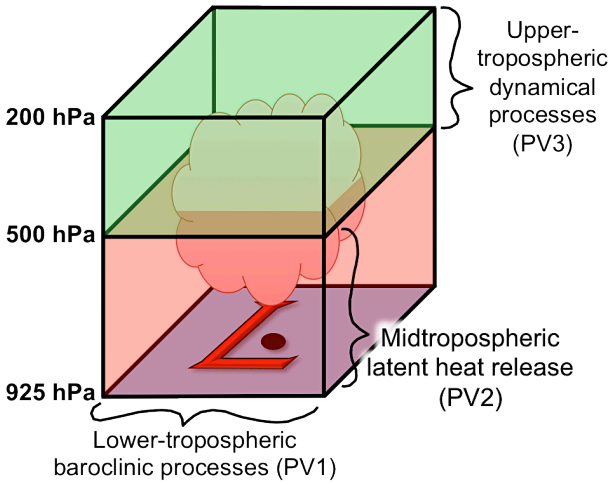

Figure 2. Schematic representation of the regions over which PV1, PV2, and PV3 are calculated. All calculations are performed within a 6° box centered over the surface cyclone (red "L"). The center of the surface cyclone is denoted by a purple dot. A region of latent heat release within the 6° box is denoted by a cloud.

The original Davis (2010) methodology used the ratio PV1/PV2 as a measure of the contribution of lower-tropospheric baroclinic processes relative to the contribution of condensation heating. With the introduction of PV3, this study introduces the ratio PV3/PV2 as a measure of the contribution of upper-tropospheric dynamical processes relative to that of condensation heating.

3. CANDIDATE CYCLONES

Only baroclinically influenced tropical cyclogenesis cases identified in McTaggart-Cowan et al. (2013) that occurred over the North Atlantic from 1979 through 2010 were considered for potential STC identification (460 candidate cyclones). The period from 1979 through 2010 was chosen to coincide with the period covered by the 0.5° CFSR dataset. North Atlantic cyclone tracks were obtained from the v03r03 edition of the International Best Track Archive for Climate Stewardship (IBTrACS) dataset (Knapp et al. 2010). In addition, North Atlantic cyclone tracks

were extended backward 36 h from their first IBTrACS position using a reverse steering flow calculation described in detail in McTaggart-Cowan et al. (2008).

McTaggart-Cowan et al. (2013) separated tropical cyclogenesis cases into one of five development pathways based on a two external forcings on the near-TC environment prior to TC formation: 1) QG forcing for ascent and 2) lower-tropospheric baroclinicity. The five development pathways identified in McTaggart-Cowan et al. (2013) include: 1) Strong TT, 2) Weak TT, 3) Trough induced, 4) Low-level baroclinic, and 5) Nonbaroclinic events. To be consistent with the NHC STC definition, only baroclinically influenced tropical cyclogenesis cases occurring in the presence of an upper-tropospheric disturbance were considered for potential STC identification, restricting the development pathways considered to those with considerable QG forcing for ascent: Strong TT, Weak TT, and Trough induced (222 candidate cyclones).

4. STC IDENTIFICATION

In order to determine the time and location of STC formation within the aforementioned subset of baroclinically influenced tropical cyclogenesis cases identified in McTaggart-Cowan et al. (2013), an objective identification technique for detecting STC formation was formulated, incorporating PV2 and PV3, and applied to the 0.5° CFSR dataset. STC formation was identified the first time ($t = t_0$) at which the following criteria were met:

1) There is a positive upper-tropospheric PV anomaly (representing an upper-tropospheric low or trough) and positive lower-tropospheric PV anomaly (representing a PV tower) over the cyclone center (i.e., PV3 > 0 and PV2 > 0 at $t = t_0$)

2) The upper-tropospheric PV anomaly begins to be eroded by midtropospheric latent heat release [i.e., $d(PV3)/dt < 0$ at $t = t_0 + 6$ h and $t_0 + 12$ h]

3) The magnitude of the upper-tropospheric PV anomaly decreases faster than the magnitude of the lower-tropospheric PV anomaly [i.e., $d(PV3/PV2)/dt < 0$ at $t = t_0$ and $t_0 + 6$ h]

4) The cyclone has not been classified by NHC as a hurricane or tropical storm at $t = t_0$, or as a tropical depression for ≥ 12 h prior to $t = t_0$

An example of the application of the objective identification technique for detecting STC formation can be seen in Fig. 3 for the case of STC Sean, which formed over the western North Atlantic in November 2011.

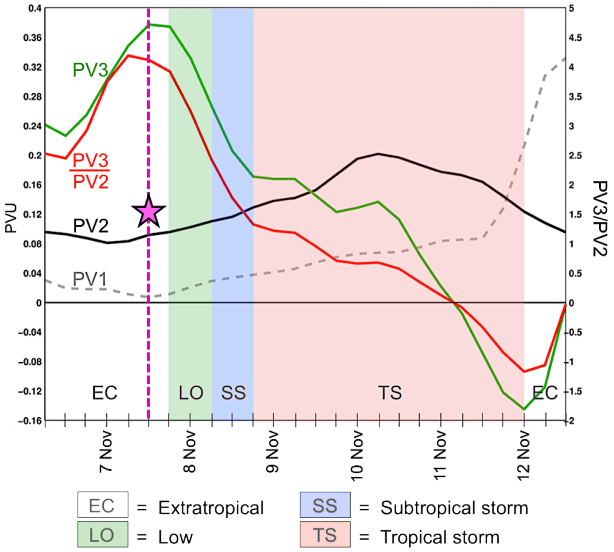

Figure 3. Graphical representation of PV1, PV2, PV3, and PV3/PV2 during the evolution of STC Sean (2011). The white, green, blue, and pink regions of the graph highlight the time periods when NHC classified Sean as an EC, low, subtropical storm, and tropical storm, respectively. The magenta line denotes the time when the objective identification technique indicated STC formation had occurred.

5. STC CLIMATOLOGY (1979–2010)

The objective identification technique for detecting STC formation was applied to the subset of baroclinically influenced tropical cyclogenesis cases identified in McTaggart-Cowan et al. (2013) that occurred over the North Atlantic during 1979–2010 in the presence of an upper-tropospheric disturbance. Of the 222 candidate cyclones, 105 were identified as STCs (~3 STCs per year). Figure 4 illustrates the intraseasonal variability associated with the location of STC formation. STC formation primarily occurs over the southern Gulf Stream and western Caribbean Sea during April–July, coinciding with the warmest sea surface temperatures (SSTs) in the North Atlantic Basin during that period (not shown). The intrusion of relatively cold upper-tropospheric air accompanying an upper-tropospheric disturbance moving over the southern Gulf Stream and western Caribbean Sea during April–July would steepen lapse rates over these regions and facilitate the development of deep convection that serves as a catalyst for STC formation. The

location of STC formation expands into the central and eastern North Atlantic during the latter half of the season (Fig. 4) as SSTs warm throughout the basin (not shown). The expansion of warm SSTs causes a larger portion of the basin to become favorable for the development of deep convection following the intrusion of relatively cold upper-tropospheric air accompanying an upper-tropospheric disturbance into the subtropics.

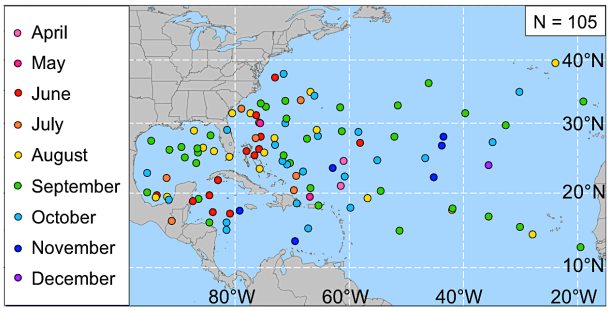

Figure 4. Locations of STC formation in the North Atlantic basin (1979–2010). The color of each dot represents the month STC formation occurred, according to the legend.

Intraseasonal variability is also associated with the frequency of STC formation in the North Atlantic basin. Figure 5 separates the 105 STCs identified in this study by the month during which they formed. STC formation occurs the most frequently in September and October, with a secondary peak in June. A seasonal minimum in STC formation is observed in July, likely due to the lack of relatively cold upper-tropospheric air impinging upon the subtropics during that month (not shown). Figure 5 also indicates that STC formation can occur from April through December, outside the range of the official North Atlantic TC season (June–November) during 1979–2010.

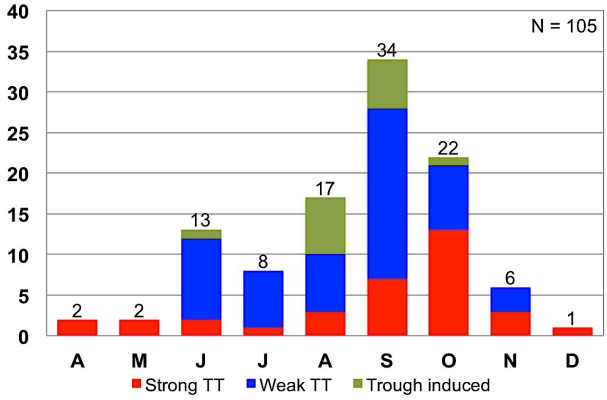

Figure 5. Frequency of STC formation in the North Atlantic basin (1979–2010) separated by month (April–December). Red, blue, and green regions represent the number of STCs classified as Strong TT, Weak TT, and Trough induced events, respectively, in McTaggart-Cowan et al. (2013).

6. CLUSTERS AND COMPOSITE ANALYSIS

A cyclone-relative composite analysis performed on subjectively constructed clusters of North Atlantic STCs identified in the 1979–2010 climatology is presented to document the structure, motion, and evolution of the upper-tropospheric features linked to STC formation. STCs included in the 1979–2010 climatology were separated into five clusters representing the most common upper-tropospheric features linked to STC formation: 1) PV Streamers, 2) Cutoffs, 3) Midlatitude Troughs, 4) Subtropical Disturbances, and 5) Debris. The percentage of STCs included in each cluster, as well as the percentage of STCs with unclassifiable upper-tropospheric precursors, is depicted in Fig. 6.

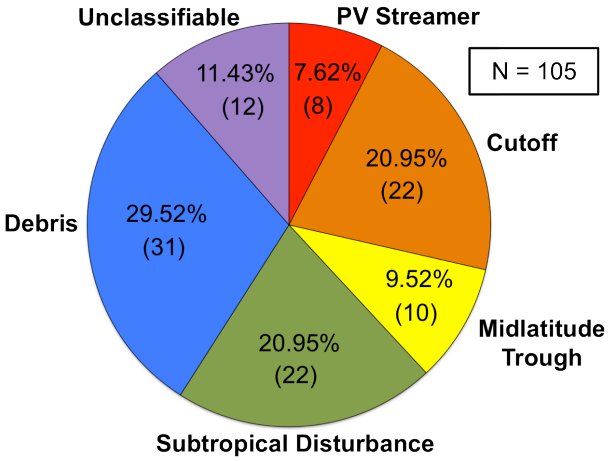

Figure 6. Distribution of 105 cases of STC formation by cluster.

STCs forming in association with a PV streamer injected into the subtropics during the initial stages of a precursor anticyclonic wave breaking (AWB) event were included in the PV Streamer cluster. In order to be included in this cluster, the PV streamer linked to STC formation must maintain a clear connection with the midlatitudes at the time of STC formation (t_0). Time-lagged cyclone-relative composites of PV on the 350 K isentropic surface reveal explosive ridge amplification, beginning at t_0 – 48 h, upstream of the position of STC formation at t_0 (not shown). Explosive ridge amplification upstream results in the formation of a downstream trough at t_0 – 24 h that stretches and thins into the PV streamer linked to STC formation by t_0 (not shown).

STCs forming in association with a region of relatively high upper-tropospheric PV cut off in the subtropics by a precursor AWB event were included in the Cutoff cluster. In order to be

included in this cluster, the region of relatively high upper-tropospheric PV must be entirely removed from the midlatitude flow at t_0. Time-lagged cyclone-relative composites of PV and winds on the 350 K isentropic surface and 200-hPa geopotential height indicate explosive ridge amplification occurring over eastern North America between t_0 – 96 h and t_0 – 48 h, resulting in the formation of a downstream trough over the western North Atlantic (Figs. 7a,b). This downstream trough continues to stretch and thin until t_0, when a region of relatively high upper-tropospheric PV on the equatorward edge of the trough is cut off in the subtropics by the poleward AWB event (Figs. 7b,c).

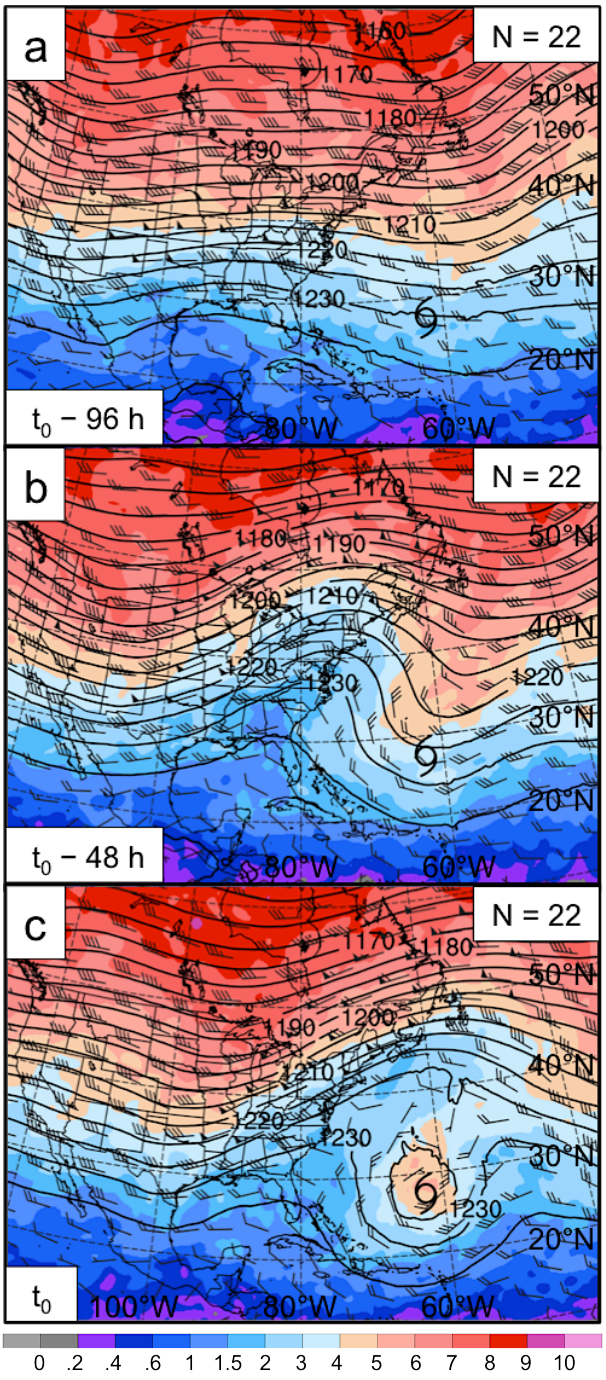

Figure 7. Time-lagged cyclone-relative composites of PV (shaded, PVU) and winds (barbs, kts) on the 350 K isentropic surface and 200-hPa geopotential height (black contours, dam) at (a) t_0 – 96 h, (b) t_0 – 48 h, and (c) t_0 for the Cutoff cluster. The cyclone symbol denotes the average position of STC formation in the Cutoff cluster at t_0.

STCs forming in association with a broad midlatitude trough that does *not* develop downstream of a precursor AWB event were included in the Midlatitude Trough cluster. Time-lagged cyclone-relative composites of PV on the 350 K isentropic surface indicate that STC formation within this cluster may be associated with multiple upper-tropospheric disturbances (not shown). The region surrounding the location of STC formation is primed for the development of deep convection by a precursor upper-tropospheric disturbance deposited into the subtropics between t_0 – 72 h and t_0 – 24 h (not shown). The approach of a broad midlatitude trough between t_0 – 24 h and t_0 focuses upward vertical motion and deep convection over the location of STC formation by providing a source of quasigeostrophic forcing for ascent (not shown).

STCs forming in association with the progression of a small-scale PV filament around the northern edge of a subtropical anticyclone were included in the Subtropical Disturbance cluster. The progressive PV filament associated with this cluster is considerably smaller in meridional extent than upper-tropospheric disturbances associated with PV Streamers, Cutoffs, or Midlatitude Troughs. This difference in meridional extent causes the cyclone-relative composites associated with Subtropical Disturbances to be less discriminating than those associated with the previous three clusters (not shown). A similar statement can be made about the cyclone-relative composites of STCs included in the Debris cluster. STCs included in the Debris cluster form in association with a disorganized region of relatively high PV deposited in the subtropics by a precursor AWB event several days prior to STC formation. In order to be included in this cluster, a disorganized region of relatively high PV must be moving westward in the subtropics on the southern edge of a broad subtropical anticyclone. The disorganized nature of PV debris results in less discriminating cyclone-relative composites than those associated with PV Streamers, Cutoffs, or Midlatitude Troughs (not shown).

7. DISCUSSION AND CONCLUSIONS

The adapted Davis (2010) methodology for STC identification presented in this paper was refined and used to construct a North Atlantic STC climatology for 1979–2010. The North Atlantic STC climatology revealed that intraseasonal variability is associated with the location and frequency of STC formation (Figs. 4 and 5). The cyclone-relative composite analysis presented in this paper reveals that North Atlantic STC formation is often associated with precursor AWB events in midlatitudes that inject regions of relatively high upper-tropospheric PV into the subtropics. Regions of relatively high upper-tropospheric PV associated with PV Streamers and Cutoffs are injected into the subtropics by upstream AWB events occurring at the time of STC formation, while regions of relatively high upper-tropospheric PV associated with Debris are injected into the subtropics by midlatitude AWB events occurring several days prior to STC formation. Questions remain unanswered concerning the influence of upper-tropospheric features linked to STC formation on the predictability of developing STCs. The author hypothesizes that some of the pathways leading to STC formation identified in this paper are inherently less predictable than others, and additional research is needed to determine the extent to which this statement is true.

The adapted Davis (2010) methodology for STC identification presented in this paper has the potential to be applied to North Atlantic cyclones in real time. The real-time application of this methodology would benefit operational forecasters and research scientists by providing them with further insight into the relative contributions of baroclinic and diabatic processes occurring during the evolution of individual cyclones, as well as by providing them with an additional tool for forecasting the TT of North Atlantic STCs.

Acknowledgments

The author would like to thank Drs. Daniel Keyser and Lance F. Bosart for their guidance in this ongoing work. This research was supported by NSF Grant AGS-0935830.

References

Beven, J. L., II, 2012: Cyclone type analysis and forecasting: A need to re-visit the issue. Preprints, *30th Conference on Hurricanes and Tropical Meteorology,* Ponte Vedra Beach, FL, Amer. Meteor. Soc., 2A.3. [Available at https://ams.confex.com/ams/30Hurricane/webprogram/Manuscript/Paper205647/2012AMSJacksonvillePaperCycloneTypes.pdf.]

Davis, C. A., 2010: Simulations of subtropical cyclones in a baroclinic channel model. *J. Atmos. Sci.*, **67,** 2871–2892.

——, and L. F. Bosart, 2003: Baroclinically induced tropical cyclogenesis. *Mon. Wea. Rev.*, **131,** 2730–2747.

——, and ——, 2004: The TT problem. *Bull. Amer. Meteor. Soc.*, **85,** 1657–1662.

Evans, J. L., and M. P. Guishard, 2009: Atlantic subtropical storms. Part I: Diagnostic criteria and composite analysis. *Mon. Wea. Rev.*, **137,** 2065–2080.

Guishard, M. P., J. L. Evans, and R. E. Hart, 2009: Atlantic subtropical storms. Part II: Climatology. *J. Climate*, **22,** 3574–3594.

Hart, R. E., 2003: A cyclone phase space derived from thermal wind and thermal asymmetry. *Mon. Wea. Rev.*, **131,** 585–616.

Knapp, K. R., M. C. Kruk, D. H. Levinson, H. J. Diamond, and C. J. Neumann, 2010: The International Best Track Archive for Climate Stewardship (IBTrACS): Unifying tropical cyclone best track data. *Bull. Amer. Meteor. Soc.*, **91,** 363–376.

McTaggart-Cowan, R., G. D. Deane, L. F. Bosart, C. A. Davis, and T. J. Galarneau, 2008: Climatology of tropical cyclogenesis in the North Atlantic (1948−2004). *Mon. Wea. Rev.*, **136,** 1284–1304.

——, T. J. Galarneau, L. F. Bosart, R. W. Moore, and O. Martius, 2013: A global climatology of baroclinically influenced tropical cyclogenesis. *Mon. Wea. Rev.*, **141,** 1963–1989.

OFCM, cited 2013: National hurricane operations plan. FCM-P12-2013. [Available online at http://www.ofcm.gov/nhop/13/pdf/FCM-P12-2013.pdf.]

Saha, S., and Coauthors, 2010: The NCEP Climate Forecast System Reanalysis. *Bull. Amer. Meteor. Soc.*, **91,** 1015–1057.